

## Supplementary material

### Construction and Application of A New Cell Electrochemical Detecting System

#### Based on the Hyposmotic Principle

Ji-Wen Cui,<sup>a</sup> Qian Wang,<sup>a</sup> Sheng Bi,<sup>b</sup> Jing Zhang,<sup>a</sup> Jin-Ling Zhu,<sup>b</sup> Ji-Guang Liu<sup>† b</sup> and Dong-mei Wu<sup>† a</sup>

<sup>a</sup>College of Pharmacy, Jiamusi University, Jiamusi, 154000, China

<sup>b</sup>College of Medicine, Jiamusi University, Jiamusi, 154000, China

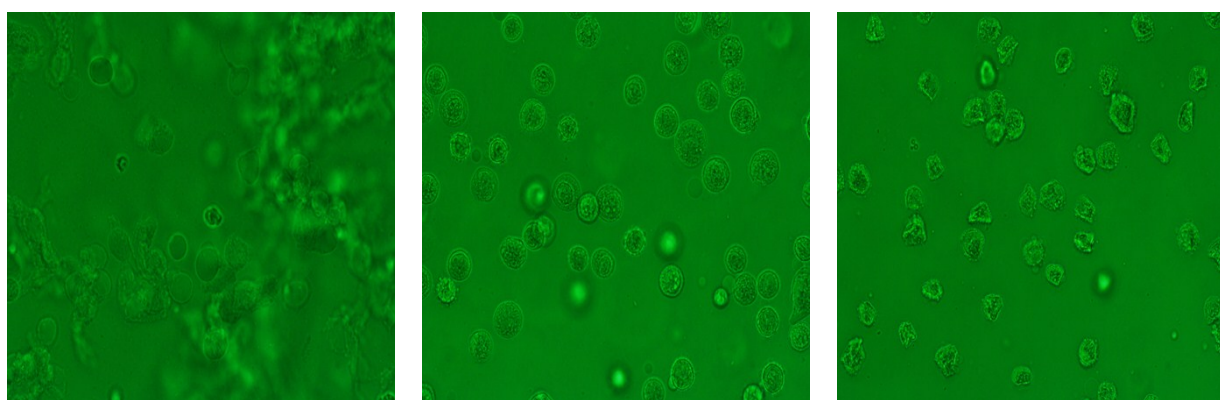


**Fig. S1** Micrographs of the fragmented MCF-7 cell suspension in the (a) hypo-CDS, (b) iso-CDS and (c) hyper-CDS. Cell concentration,  $5 \times 10^6$  cells  $\text{mL}^{-1}$ .

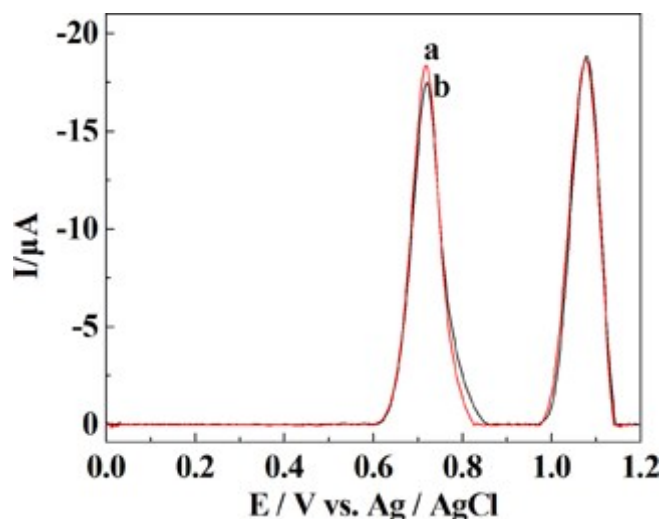


**Fig. S2** Baseline-corrected LSV of the fragmented MCF-7 cell suspension (a) with and (b) without ultrasonic treatment. Cell concentration,  $5 \times 10^6$  cells  $\text{mL}^{-1}$ .

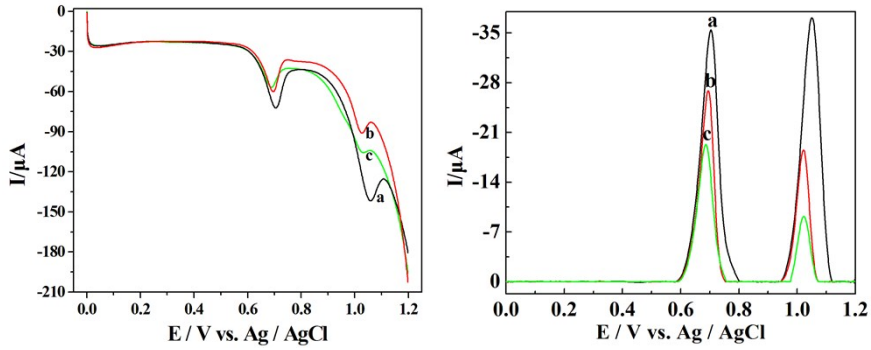


Fig. S3 The original figure and baseline-corrected of LSVs of the fragmented MCF-7 cell suspension in the (a) hypo-CDS, (b) iso-CDS and (c) hyper-CDS. Cell concentration,  $5 \times 10^6 \text{ cells mL}^{-1}$ .

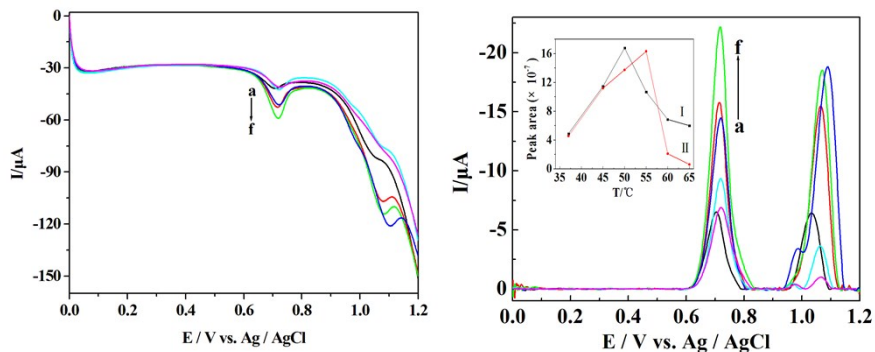


Fig. S4 (A) The original figure and baseline-corrected of LSVs in the hypo-CDS with the different fragmented temperature: a)  $37 \text{ }^\circ\text{C}$ , (b)  $65 \text{ }^\circ\text{C}$ , (c)  $60 \text{ }^\circ\text{C}$ , (d)  $45 \text{ }^\circ\text{C}$ , (e)  $55 \text{ }^\circ\text{C}$ , and (f)  $50 \text{ }^\circ\text{C}$ .

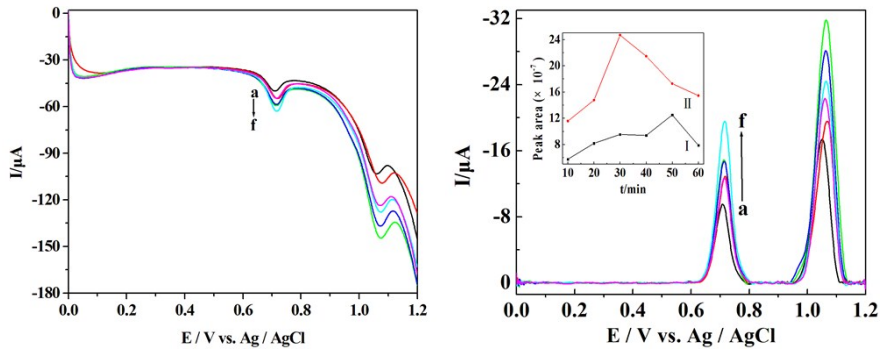


Fig. S4 (B) The original figure and baseline-corrected of LSVs in the hypo-CDS with the different fragmented time: (a) 10 min, (b) 60 min, (c) 20 min, (d) 40 min, (e) 30 min, and (f) 50 min. Cell concentration,  $5 \times 10^6 \text{ cells mL}^{-1}$ .

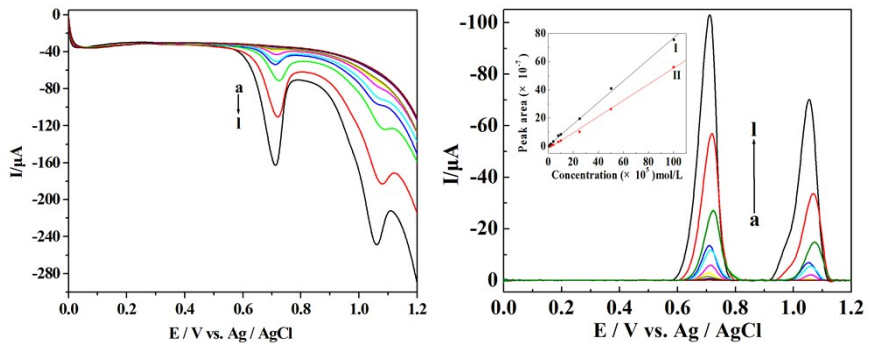


Fig. S5 (A) The original figure and baseline-corrected of LSVs in the hypo-CDS at different concentration,(a)  $1.0 \times 10^4$ , (b)  $2.5 \times 10^4$ , (c)  $5.0 \times 10^4$ , (d)  $1.0 \times 10^5$ , (e)  $2.0 \times 10^5$ , (f)  $4.0 \times 10^5$ , (g)  $8.0 \times 10^5$ , (h)  $1.0 \times 10^6$ , (i)  $2.5 \times 10^6$ , (j)  $5.0 \times 10^6$ , (k)  $8.0 \times 10^6$ , and (l)  $1.0 \times 10^7$  cells  $\text{mL}^{-1}$ .

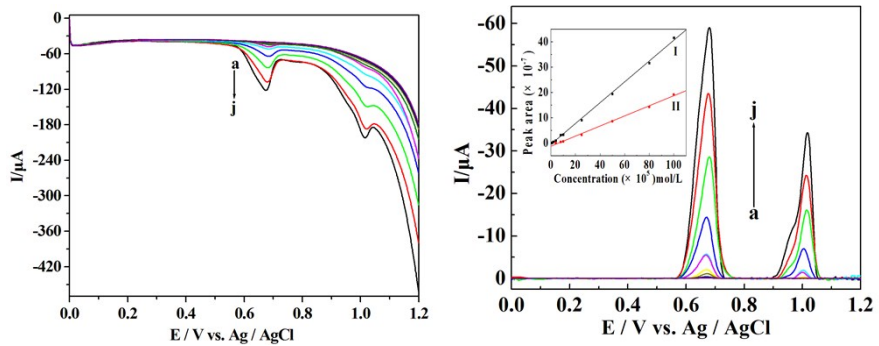


Fig. S5 (B) The original figure and baseline-corrected of LSVs in the hyper-CDS at different concentration,(a)  $5 \times 10^4$ , (b)  $1.0 \times 10^5$ , (c)  $2.0 \times 10^5$ , (d)  $4.0 \times 10^5$ , (e)  $8.0 \times 10^5$ , (f)  $1.0 \times 10^6$ , (g)  $2.5 \times 10^6$ , (h)  $5.0 \times 10^6$ , (i)  $8.0 \times 10^6$ , and (j)  $1.0 \times 10^7$  cells  $\text{mL}^{-1}$ .

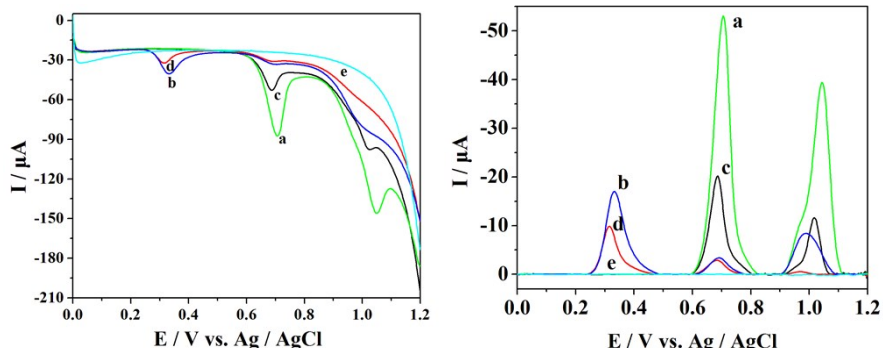


Fig. S6 The original figure and baseline-corrected of LSVs in the hypo-CDS (a) without and (b) with XO; LSVs in the hyper-CDS (c) without and (d) with XO; (e) XO.

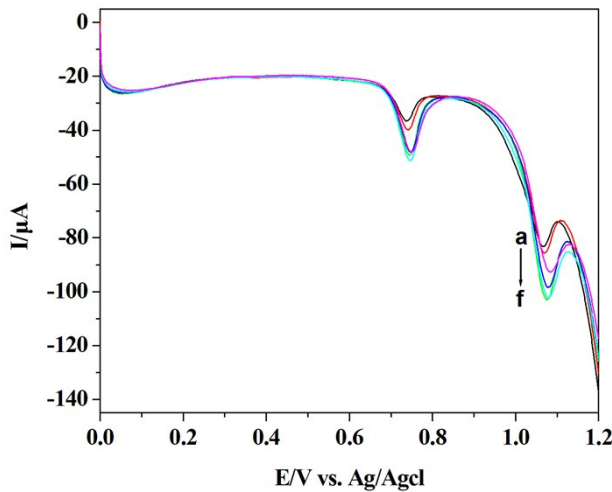


Fig. S7 LSVs in the iso-CDS with the different fragmented time: (a) 10 min, (b) 20 min, (c) 60 min, (d) 50 min, (e) 40 min, and (f) 30 min.

**Table S1** The peak area and concentration of purine in the fragmented MCF-7 cell suspension.

	G/X	A/H	G	X	A	H
S <sup>a</sup> (×10 <sup>-7</sup> )	13.59(±0.384)	6.46(±0.283)	2.13(±0.041)	11.46(±0.384) <sup>e</sup>	0.28(±0.000)	6.46(±0.312) <sup>e</sup>
S <sup>b</sup> (×10 <sup>-7</sup> )	38.06(±0.384)	31.92(±0.283)	2.60 (±0.041)	35.46(±0.384) <sup>e</sup>	8.30(±0.000)	23.62(±0.312) <sup>e</sup>
C <sup>c</sup> (μmol L <sup>-1</sup> )			3.785	10.174	2.468	10.787
C <sup>d</sup> (μmol L <sup>-1</sup> )			4.175	31.973	11.469	33.883

<sup>a</sup> Peak area for heated fragmented, <sup>b</sup> Peak area for composite fragmented, <sup>c</sup> Calculated concentration for heated fragmented, <sup>d</sup> Calculated concentration for composite fragmented, <sup>e</sup>  $S_X = S_{G/X} - S_G$ ,  $S_H = S_{A/H} - S_A$ .